Fault Detection and Diagnosis of IC Engine based Power Trains by IAS Analysis

Yuandong Xu, Yuliang Yun, Fengshou Gu, Andrew D. Ball

Fault Detection and Diagnosis of IC Engine Power Trains Based on IAS Analysis

Yuandong Xu[1], Yuliang Yun[2], Fengshou Gu[1], Andrew D. Ball[1]
[1]Centre for Efficiency and Performance Engineering, University of Huddersfield, UK
[2]College of Mechanical and Electrical Engineering, Qingdao Agricultural University, China
yuandong.xu@hud.ac.uk

Abstract

Internal combustion (IC) engine based power trains are common transmissions in different industries such as trains, standby power supply and marine drives. Conventional vibration based monitoring often needs a considerable number of sensors because of large layout of the system, which is cost-intense and difficult to operation. This study focuses on developing a cost-effective approach to monitoring such a large system using one or two channels of instantaneous angular speed (IAS) measurements. It models the powertrain system as a flexible nonlinear rotor and characterises IAS responses at different measurement positions when the system is under different faults such as misfires, coupling defects, lubricant deterioration and impeller defects. The results show that it is feasible to use a fewer of IAS channels to monitor the entire system, but its performance depends largely on the sensor locations and data processing methods. The simulation studies based on the developed torsional model with 8 degree of freedom demonstrates that the IAS signals at the pulley wheel achieves the best detection results for the misfires in different cylinder of the 4 cylinder engine powertrain.

Keywords: IAS, power train rotor system, misfire, fault detection, model

1 Introduction

The reciprocating machines are the vital components of the machinery and engines are one of typical reciprocating machines. The engine based powertrains are widely used in the fields of vehicles, ships, power generation. Misfire is a common engine fault, which occurs frequently in IC engines. Many reasons can lead to combustion faults, such as spark plug failure, cracked distributor caps, broken head gaskets, lean fuel/air mixture, compression lack, exhaust recirculation, and improper valve timing. Engine misfire is responsible for power loss, poor fuel economy, and more exhaust emission. Consequently, it is necessary to detect and solve the problem to maintain the performance and reduce the pollution. However, engine misfire is difficult to detect and diagnose [33], especially for multi-cylinder engines.

Vibration and instantaneous angular speed (IAS) angular speed are the common tools in the field of misfire detection. This paper mainly focuses on the torsional vibration or IAS based investigation of fault detection and diagnosis. Torsional vibration is the oscillation of the angular motions that occurs along the rotating elements, for example, gears trains, shafts, or clutches. Boysal and Rahnejat [1] built a detailed multi-body numerical nonlinear dynamic model of a single cylinder internal combustion engine to analyse the torsional vibrations of the crankshaft and the whirl of journal bearings. Remond [3] introduced that the encoder technique is a cheap and easy way to implement transmission error measurement or torsional vibration measurement on real mechanical systems with high precision and sufficient reliability. Instantaneous angular speed was successfully employed for torsional vibration analysis. In order to discriminate early faults of the rotating machine, the accuracy of the measurement of IAS is highly demanded [4]. The IAS spectra directly associated with the engine firing frequency can be utilized to estimate engine loading condition [5]. Gu [6] et al. investigated the instantaneous angular speed (IAS) signal

characteristics to detect and diagnose faults of piston engines. Sasi [7] demonstrated the use of IAS to monitor electric motors. Feldman and Seibold [8] investigated the detection of the size and location of damage in a rotor system using IAS. Charles [9] et al used IAS signal, representing the torsional vibration of the crankshaft, to diagnose the faults of diesel combustion. These investigations show that IAS is useful for the condition monitoring of a wide variety of rotating machines. Hill [10] introduced some torsional vibration failure cases and presented the torsional modelling methods in detail. Mendes, Meirelles and Zampieri [11] considered the rubber and damper on the crankshaft to model a six-cylinder diesel engine and the torsional vibration from the model was similar with the experimental value. Misfire in an IC engine is a continuous problem and many researchers have applied various approaches to detect misfire. Kuroda et al. [12] proposed digital filtering technology of crank speed measurement to detect misfire. Kiencke [13] used Kalman filter to build an engine model to estimate the combustion torque from angular velocity measurement.

The aforementioned research works successfully achieved accurate diagnosis of rotating machine faults by using IAS measurements. However, the research on the optimal measurement position has not been studied, which can lead to a cost-effective and efficient detection solution for the engines. Hence, this paper aims to investigate and determine the optimal sensor position for accurate misfire fault detection based on the torsional vibration model of a powertrain. The remaining contents of the paper are arranged as follows. The Section 2 introduces the model development of a 4 cylinder diesel engine based powertrain system, and in the following section, the model based simulation studies is evaluated to determine the optimal position for acquiring the IAS signals, which can detect and diagnose the misfire faults effectively and efficiently. The conclusions are drawn in the last part.

2 Model Development

2.1 Engine Rig Facilities

The test engine is under the control of a CP Cadet V12 control and data logging system. It is integrated with high speed data acquisition (cylinder combustion analysis), engine management and control system and full vehicle simulation. The transient conditions are controlled by six of the proportional integral derivative loops.
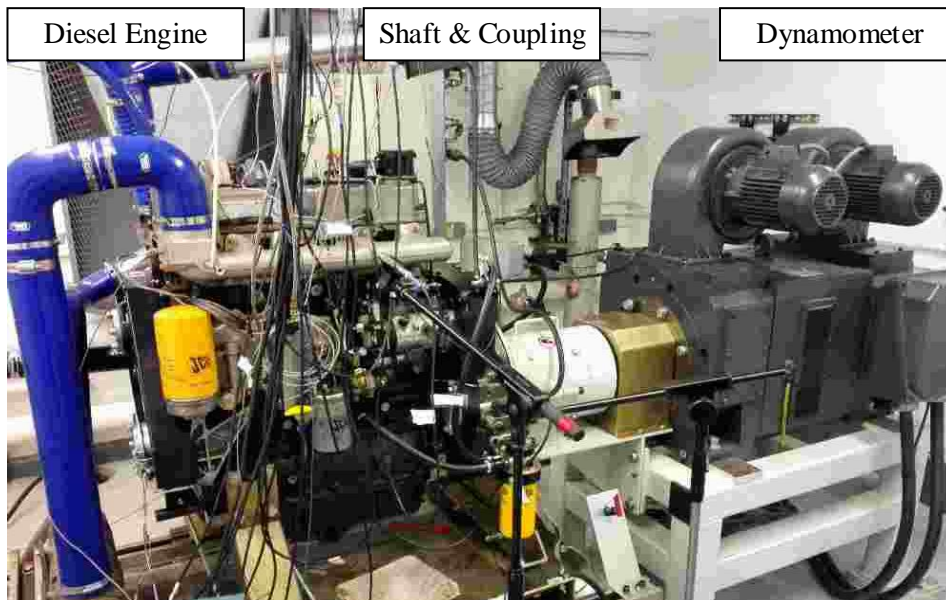

Figure 1: Layout of the engine test rig

The specifications of JCB444 T2 diesel engine are shown in Table 1.

Technical parameters	Technical data
Engine type	Diesel engine

Number of Cylinders	4
Firing order	1-3-4-2
Maximum torque	425 Nm @ 1300 rpm
Maximum power	74.2 kW @ 2200 rpm
Compression ratio	18.3:1

Table 1: Diesel engine specifications

In order to obtain the operation information of the engine, a data acquisition (DAQ) system was set up to acquire the data sets including vibration, IAS, in-cylinder pressure. The cylinder pressure transducer is placed in the cylinder 1 and the DAQ facilities are listed in detail in the Table 2.

Equipment	Model	Key specifications
Optical switch	OPB900W55Z	250kBaud
Hall effect sensor	IME12-02 BPSZ	2kHz
Encoder	376836-20	1024ppr
Cylinder pressure	112A05	1.129pC/psi
DAQ device	YE6323B	16CH, 96kHz

Table 2: Equipment on the engine test rig

In the experiment, the test engine was operated at different loads and speeds. The engine was running at two speeds 1300rpm and 1600rpm and two loads 0Nm and 105Nm were applied at each speed. In order to investigate the engine dynamics at misfire conditions, a manual fault of 100% misfire at cylinder 1 is set up to obtain the faulty signals. At each operating point, cylinder pressure signals along with others are acquired simultaneously for three records of 30 seconds at sampling rate 96kHz when the engine operates at steady conditions.

2.2 Torsional Model Development

In order to study the torsional vibration of the engine based rotor system, a torsional vibration model is developed to simulate the dynamic responses, which is employed to investigate the effective and cost-effective diagnosis approaches. The engine based power train system can be represented by a lump model to investigate the torsional vibration responses, which is shown in the Figure 2. The torsional model has 10 degree of freedom, including the pulley wheel, 4 cylinders, the flywheel, the flexible coupling, and the dynamometer.

Figure 2: Schematic of the torsional model

The torsional vibration model of the system can be derived and expressed in matrix form as

$$\mathbf{I}\{\ddot{\theta}\} + \mathbf{C}\{\dot{\theta}\} + \mathbf{K}\{\theta\} = \mathbf{T_T} \tag{1}$$

where, $\boldsymbol{\theta} = [\theta_1\ \theta_2 \cdots \theta_8]^T$ is the torsional vibration vector; $\mathbf{I}$, $\mathbf{C}$, $\mathbf{K}$ are the matrixes of the moment of inertia, torsional damping, and torsional stiffness, which can be expressed as follows.

$$\mathbf{I} = \text{diag}([I_1, I_2, \cdots I_8]) \tag{2}$$

$$\mathbf{C} = \begin{bmatrix} c_1 & -c_1 \\ -c_1 & c_1 + c_2 & -c_2 \\ & -c_2 & c_2 + c_3 & -c_3 \\ & & -c_3 & c_3 + c_4 & -c_4 \\ & & & -c_4 & c_4 + c_5 & -c_5 \\ & & & & -c_5 & c_5 + c_6 & -c_6 \\ & & & & & -c_6 & c_6 + c_7 & -c_7 \\ & & & & & & -c_7 & c_8 \end{bmatrix} \tag{3}$$

$$\mathbf{K} = \begin{bmatrix} k_1 & -k_1 \\ -k_1 & k_1 + k_2 & -k_2 \\ & -k_2 & k_2 + k_3 & -k_3 \\ & & -k_3 & k_3 + k_4 & -k_4 \\ & & & -k_4 & k_4 + k_5 & -k_5 \\ & & & & -k_5 & k_5 + k_6 & -k_6 \\ & & & & & -k_6 & k_6 + k_7 & -k_7 \\ & & & & & & -k_7 & k_8 \end{bmatrix} \tag{4}$$

The torque vector at the right side of the model equation can be expressed as

$$\mathbf{T_T} = \begin{bmatrix} 0, T_{g1}, T_{g2}, T_{g3}, T_{g4}, 0, 0, T_e \end{bmatrix} \tag{5}$$

where, the $T_{g1}, T_{g2}, T_{g3}, T_{g4}$ are the gas torques from the combustion and T_e is the external load from the dynamometer.

The parameters used in this model is listed in the Table 3.

Inertia (kgm^2)	Stiffness ($10^6 Nm/rad$)	Damping ($Nm/rad/s$)
$I_1 = 0.025$	$k_1 = 0.1$	$c_1 = 10.37$
$I_2 = 0.027$	$k_2 = 1.37$	$c_2 = 17.98$
$I_3 = 0.027$	$k_3 = 1.37$	$c_3 = 17.98$

$I_4 = 0.027$	$k_4 = 1.37$	$c_4 = 17.98$
$I_5 = 0.027$	$k_5 = 2.03$	$c_5 = 25.941$
$I_6 = 0.954$	$k_6 = 0.01$	$c_6 = 80$
$I_7 = 0.58$	$k_7 = 0.01$	$c_7 = 80$
$I_8 = 0.059$	-	-

Table 3: Model parameters

The modal parameters can be obtained from the inertia and stiffness matrix and the first 5 modes of the model are listed in Table 4. These resonant responses can lead to the inaccurate detection and diagnosis when using the IAS signals. In the simulation studies, the resonance in the torsional vibration will be removed to secure the unbiased evaluation of the diagnostic performance.

Modal Order	Natural Frequency (Hz)
1st	25
2nd	69.1
3rd	275..2
4th	511.7
5th	1229.1

Table 4: Natural frequencies

The parameters of the torsional model are determined and then, the external torques from the combustion and load are calculated to drive the model for obtaining the IAS at different positions.
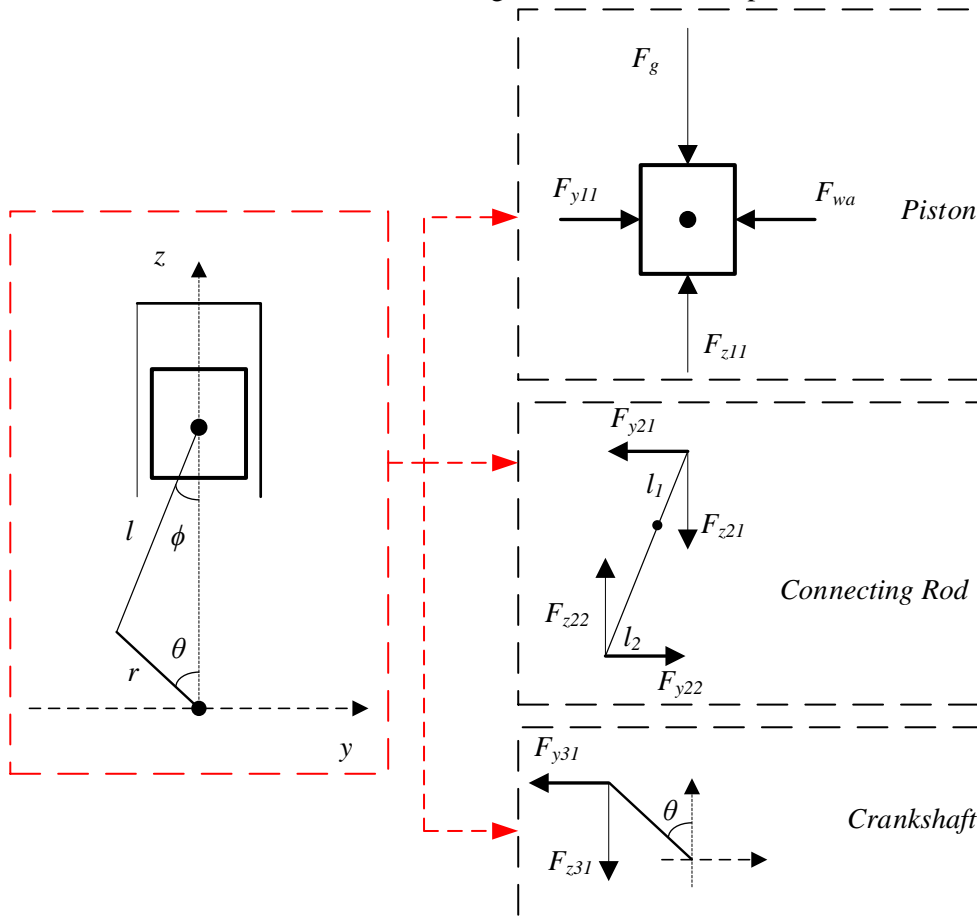
Figure 3: Schematic diagram of forces on components of the crank-piston system

5

Figure 3 depicts the forces on the elements of the crank-piston system. The torques of the rotor model consist of the gas torque and the load torque and the friction forces are not considered in this model. Suppose the external load of the engine system is constant, the variation of the torques are mainly from the variation of the in-cylinder pressure. The gas pressure on the cylinder generates the power forces for the whole rotating system and the forces on the elements of the crank-piston system [14] are shown in Figure 3.

Finally, the gas torque for the single-cylinder engine is presented as

$$T_g = \frac{[F_g - m_p r \dot{\theta}^2 (\cos\theta + r/l \cos 2\theta)] r/l \sin\theta}{\sqrt{1 - (r/l \sin\theta)^2}} (l\cos\phi + r\cos\theta) \tag{6}$$

where, F_g is the gas force produced by the cylinder pressure; m_p is the piston mass; r and l are the length of the crank and the connecting rod respectively; θ and $\dot{\theta}$ are the crankshaft rotating angle, angular speed and angular acceleration.

For a straight-four engine, the torsional torque is varying based on the firing order. The torsional forces can be easily derived from the motion of the crank-piston system, however the arguments related with movement of the piston and crankshaft are not easy to obtain. Therefore, differential equations based on the first principle model are solved by using ode functions. The model is driven by the experimental cylinder pressure. The discrete pressure waveform is not adequate for the simulation, and therefore a proper fitting of the pressure curve is produced in MATLAB for numerical solutions. Figure 4 shows the fitted cylinder pressure curves at health and misfire conditions.
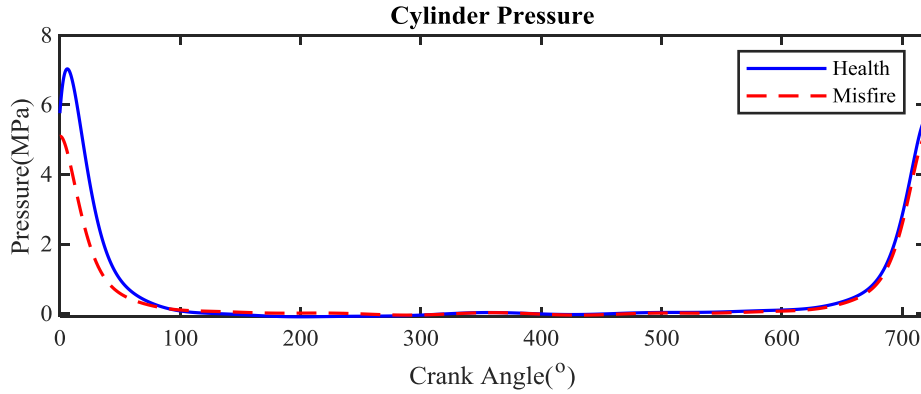

Figure 4: Cylinder pressure at health and misfire conditions

The resultant torques on the cranks are the combination of the torque from the fuel combustion and the moment of inertia. As shown in Figure 5, the torque on one crank at the health condition is denoted by the red dashed line. The resultant torque at each crank will be applied to drive the model according to the corresponding cylinder firing order.
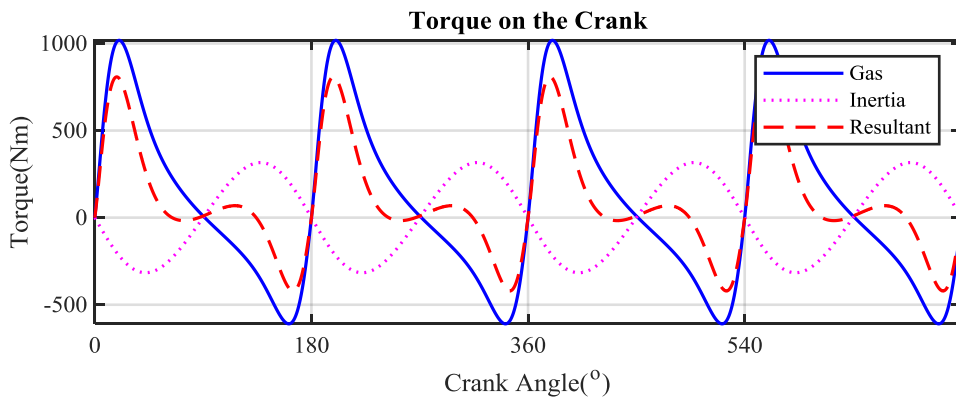

Figure 5: Torque on the crank

3 Model based Investigation

3.1 Verification of the Torsional Model

The simulation results of the IAS at the pulley wheel, first cylinder, flywheel, coupling and dynamometer are displayed in the Figure 6 (a). The results in the figure is based on the engine running at the speed of 1600rpm and load of 105Nm and the following results are mainly explained by using this running condition. The IAS oscillation is the speed variation after deducting the average engine speed at different crank angles in an engine cycle. The simulation results in both angle and frequency domain show that the responses at the flywheel, coupling and dynamometer are more smooth than that at the pully wheel and cylinders, which is mainly due to the large moment of inertia of the flywheel and the high damping of the coupling.
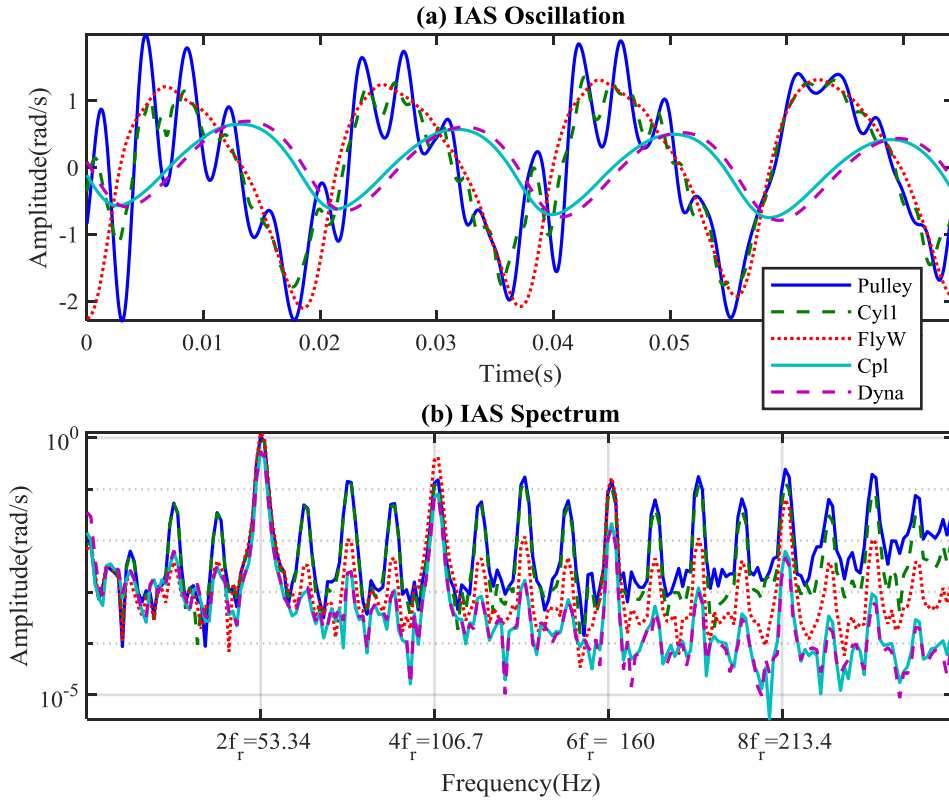
Figure 6: IAS of pulley wheel, cylinder 1, flywheel, coupling, and dynamometer

Figure 7 shows the order spectra of the simulated and experimental IAS signals at the pulley wheel when the engine runs at the speed of 1600rpm and the load of 105Nm. The comparation results show that the established model generates highly identical outputs with the experimental signals. The comparation can verify the accuracy of the developed torsional model, which then allows the thoroughly investigation of the IAS based detection and diagnoses.
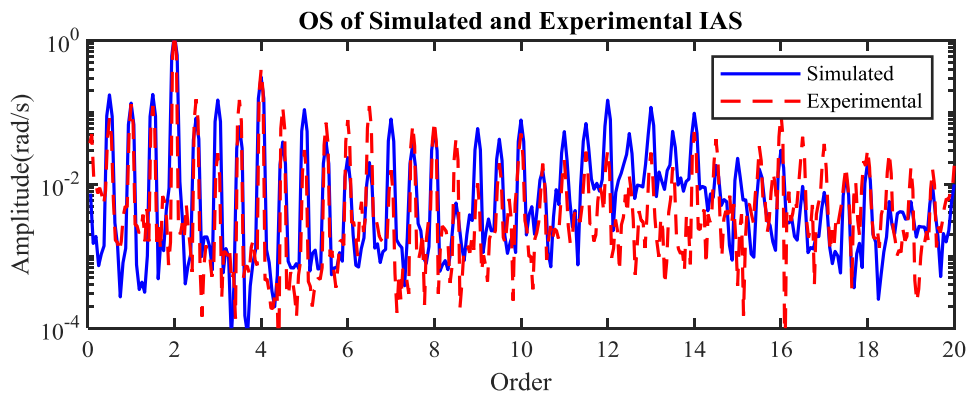

Figure 7: Order spectra of the simulated and experimental IAS at the pulley wheel

3.2 Simulation Studies of Misfire and Coupling Faults

7

The introduced faults of the engine are the 100% misfire of each cylinder and the improper stiffness of the coupling. The differences of the IAS outputs are used to demonstrate the faults induced IAS variation. Figure 8 shows the IAS signals obtained at the pulley wheel, cylinder 2, flywheel and dynamometer respectively. If the misfire fault occurs in the cylinder 1, the combustion stroke cannot generate power outputs for driving the system and consequently, the instantaneous angular speed after the desired combustion event is lower than that in the health condition. It is obvious that the cylinder 1 misfire results in the speed decrease at the crank angle of 90° from all the responses at 8 DOF. In the same manner, the case of cylinder 2 has the identical responses at the crank angle of 630° due to the engine firing order of 1-3-4-2. The angular domain results can easily distinguish the fault cylinder and evaluate the fault severity.
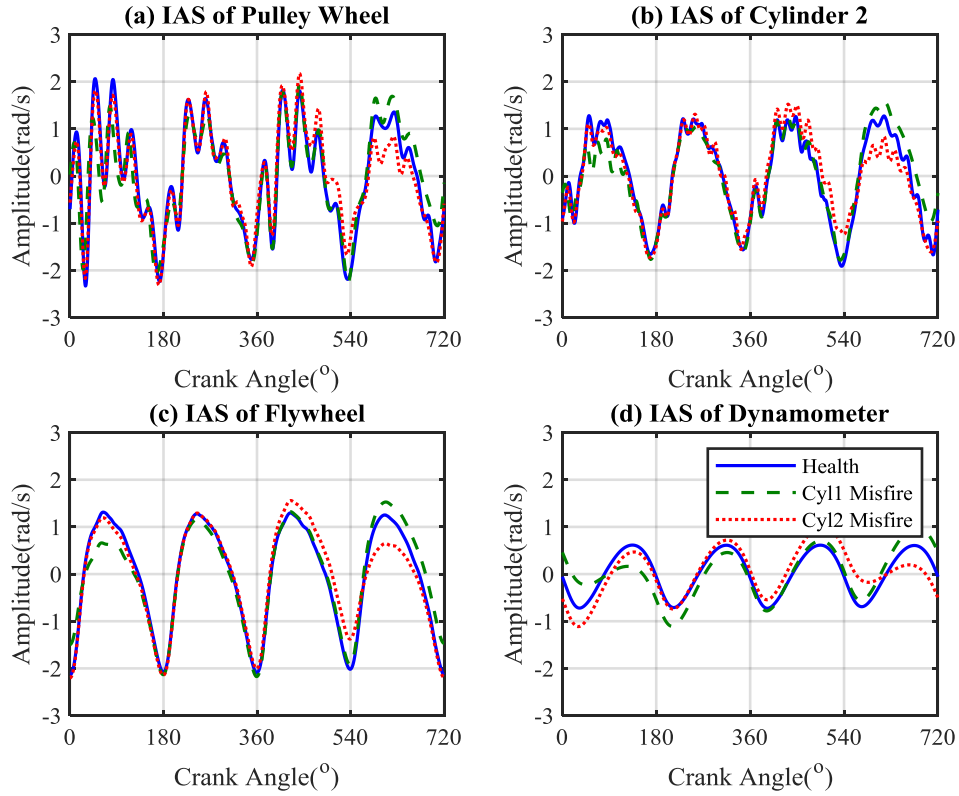

Figure 8: IAS signals in the angular domain

The order spectra (OS) from the angular IAS signals are depicted in the Figure 9. The peaks excluding the firing frequency are higher than the health case, of which the reason is that the misfire faults make the combustion uneven and hence generate more oscillation of the shaft rotation.
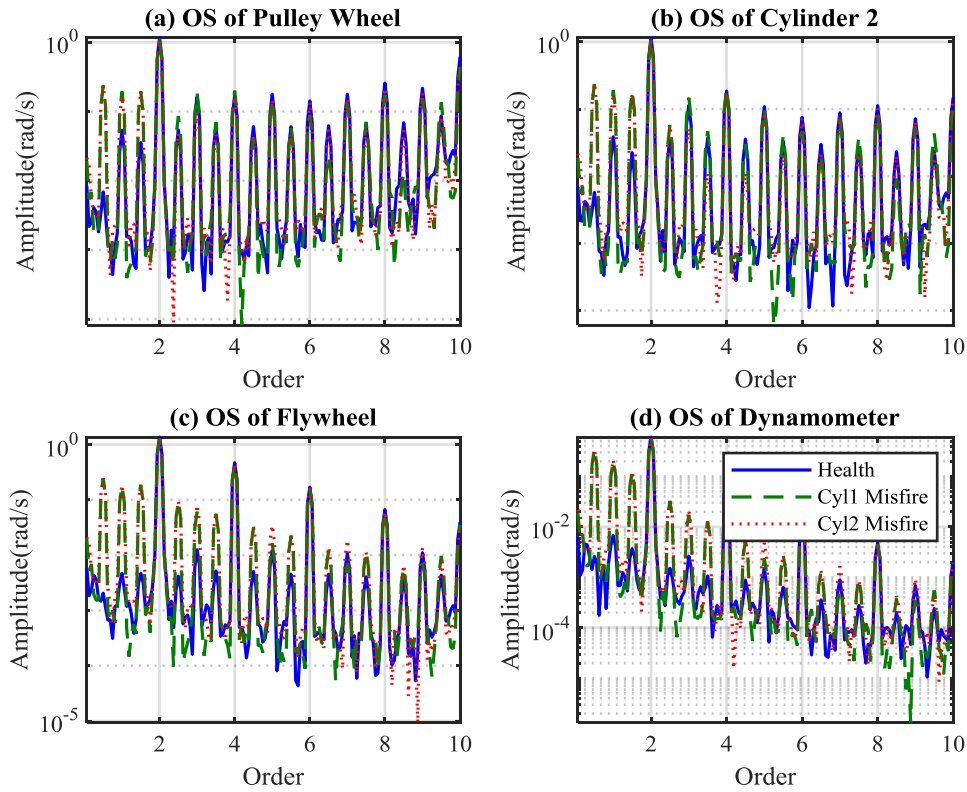
8

Figure 9: Order spectrum of the IAS signals

The IAS responses are unavoidably interfered by the torsional resonance of the power train system and consequently, the comparison of the IAS from 8 DOF has to remove the resonance behaviour. In this way, the diagnostic results can be comparable in regard to the determination of the optimal measurement position on the power train system. The theoretically modal parameters are listed in the Table 4 and hence, the responses around the natural frequencies cannot be taken into account, which are significantly interfered by the system resonance. The frequency components around the natural frequencies in the angular IAS signals are removed by designed 5 bandpass filters which have a bandwidth of 20Hz centred at each natural frequency. Then, the IAS residues in the angular domain are obtained by the difference between the IAS at health and faulty conditions when the engine runs at the speed of 1300rpm and the load of 105Nm. The root mean square (RMS) values of the residual signals are displayed in the Figure 10 (a) and the differences of the IAS at the pulley wheel are more pronounced at four misfire cases. Both results in the angular and frequency domain are compared for finding the effective measurements. As explained that the resonance has to be eliminated to accurately evaluate the performance of the IAS signals, the OS residues are extracted by summing up peak values at the orders of 0.5 to 20, which is exclusive of the resonant behaviour around the natural frequencies with a bandwidth of 20Hz. Similarly, the order spectrum residues of the IAS signals lead to the same conclusion that the position at the pulley wheel shows best performance in diagnosing the misfire and coupling faults.
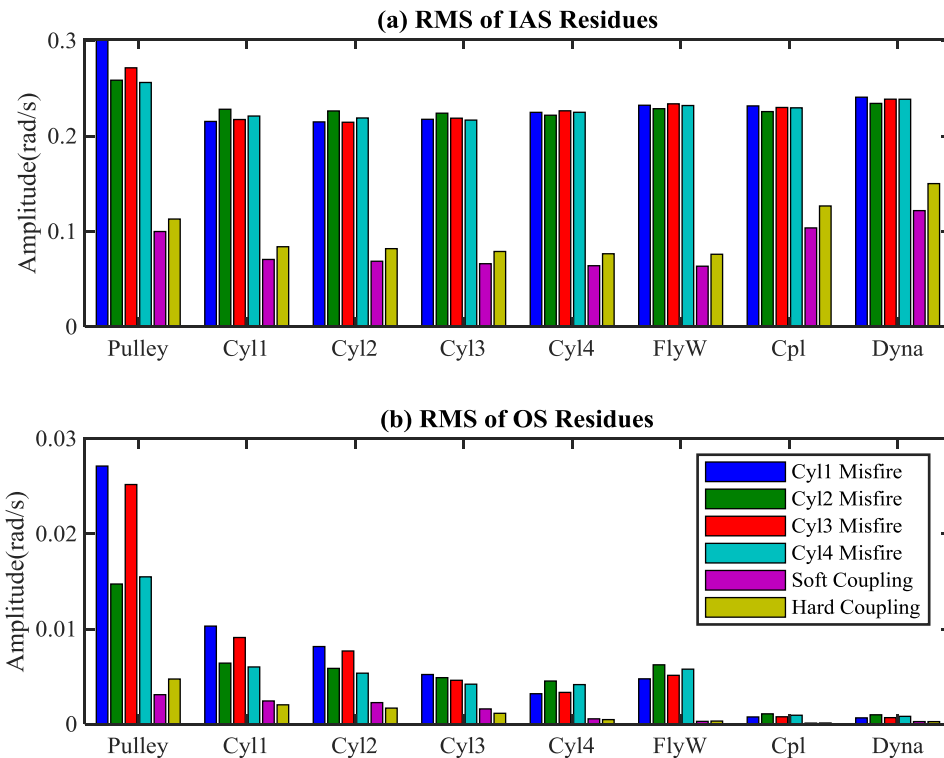
Figure 10: Differences of IAS at 8 DOF at 1300rpm and 105Nm

Figure 11 depicts the IAS residues in both the angular and frequency domain when the engine runs at the speed of 1600rpm and the load of 105Nm. The results show that the IAS signals at the pulley wheel are more effective than the others.
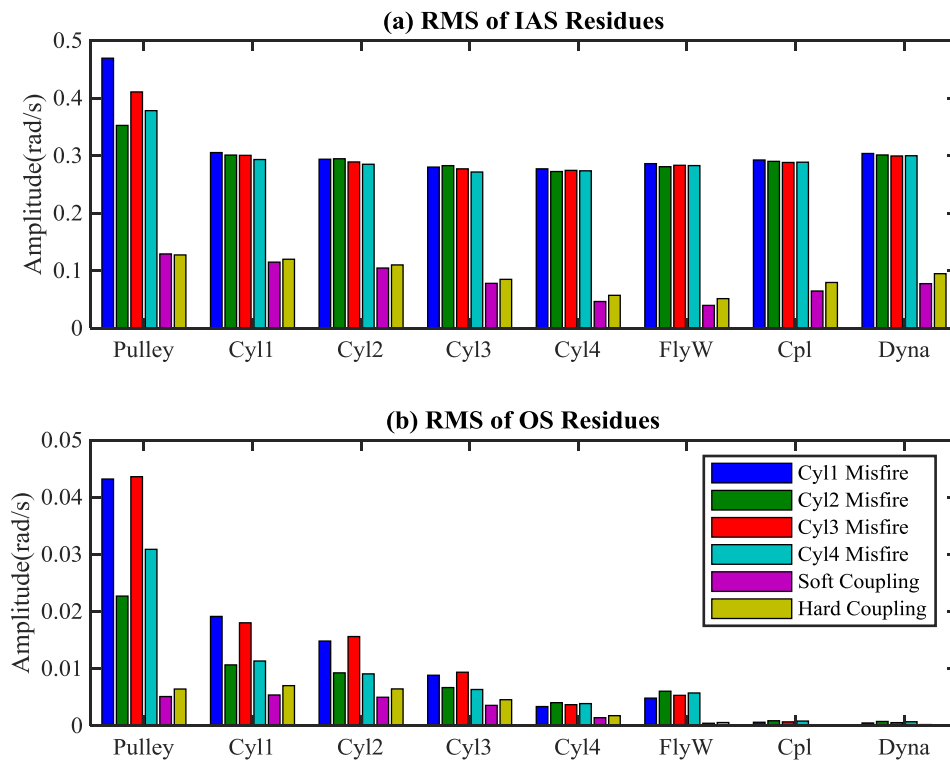

Figure 11: Differences of IAS at 8 DOF at 1600rpm and 105Nm

The meaningful positions for measuring the IAS signals are exclusive of the internal cylinders. In general, the IAS can be acquired from the pulley wheel, flywheel, coupling and the dynamometer. The results of the simulation studies show that the pulley wheel is an optimum position for achieving the most

effective diagnoses of the misfire and coupling faults. The torsional model was developed by referring to a 4 cylinder diesel engine based power train system. The 4 cylinder engine is small compared with the large and multiple cylinder engines, which results in the response at the pulley wheel is sensitive to the running conditions because the high stiffness of the crankshaft and the small moment of inertia of the pulley wheel. Due to the compensation of the energy stored in the flywheel, the IAS oscillates gently from the position of the flywheel. Consequently, the IAS signals obtained from the flywheel, coupling and dynamometer have more smooth waveforms. Hence, the performance of the IAS measured at the pulley wheel is considered to be optimal.

4   Conclusions

This paper focuses on the investigation of the detection and diagnoses performance of the IAS measurements in the IC engine power trains. This study can pave the way to the development of the effective and cost-effective approaches for monitoring the working conditions of the engine powertrains. A torsional model with 8 DOF was developed to obtain the IAS signals at different measurement positions, which was verified by the experimental IAS results. The accurate model allows the effective comparation of the IAS responses under different working conditions. The simulation results show that the IAS measured at the pulley wheel is more efficient to detect and diagnose the misfire faults at different cylinders and the coupling faults with improper stiffness.

The conclusion is drawn based on the simulation studies of a 4 cylinder engine model. The results can be different if the target is a large engine. In the future studies, the influence of the large engines as well as the signal to noise ratio of the measurements will be taken into account to give more valuable recommendations for the development of the effective and cost-effective online methods for the engine based powertrains.

Acknowledgments

References

[1]   A. Boysal and H. Rahnejat, 'Torsional vibration analysis of a multi-body single cylinder internal combustion engine model', *Applied Mathematical Modelling*, vol. 21, no. 8, pp. 481–493, Aug. 1997.

[2]   Y. Kang, G.-J. Sheen, M.-H. Tseng, S.-H. Tu, and H.-W. Chiang, 'Modal Analyses and Experiments for Engine Crankshafts', *Journal of Sound and Vibration*, vol. 214, no. 3, pp. 413–430, Jul. 1998.

[3]   D. Remond, 'Practical performances of high-speed measurement of gear transmission error or torsional vibrations with optical encoders', *Meas. Sci. Technol.*, vol. 9, no. 3, p. 347, 1998.

[4]   F. Gu, I. Yesilyurt, Y. Li, G. Harris, and A. Ball, 'An Investigation of the Effects of Measurement Noise in the Use of Instantaneous Angular Speed for Machine Diagnosis', *Mechanical Systems and Signal Processing*, vol. 20, no. 6, pp. 1444–1460, Aug. 2006.

[5]   T. R. Lin, A. C. Tan, L. Ma, and J. Mathew, 'Condition monitoring and fault diagnosis of diesel engines using instantaneous angular speed analysis', *Proceedings of the Institution of Mechanical Engineers, Part C: Journal of Mechanical Engineering Science*, p. 0954406214533253, Apr. 2014.

[6]   F. Gu, P. J. Jacob, and A. D. Ball, 'Non-parametric models in the monitoring of engine performance and condition: Part 2: Non-intrusive estimation of diesel engine cylinder pressure and its use in fault detection', *Proceedings of the Institution of Mechanical Engineers, Part D: Journal of Automobile Engineering*, vol. 213, no. 2, pp. 135–143, Feb. 1999.

[7]   Ahmed Yousef Ben Sasi, Fengshou Gu, Bradley Payne, and Andrew Ball, 'Instantaneous Angular Speed Monitoring of Electric Motors', *J of Qual in Maintenance Eng*, vol. 10, no. 2, pp. 123–135, Jun. 2004.

[8] M. Feldman and S. Seibold, 'Damage Diagnosis of Rotors: Application of Hilbert Transform and Multihypothesis Testing', *Journal of Vibration and Control*, vol. 5, no. 3, pp. 421–442, 1999.

[9] P. Charles, J. K. Sinha, F. Gu, L. Lidstone, and A. D. Ball, 'Detecting the Crankshaft Torsional Vibration of Diesel Engines for Combustion Related Diagnosis', *Journal of Sound and Vibration*, vol. 321, no. 3–5, pp. 1171–1185, Apr. 2009.

[10] C. Hill, 'Guidelines for Preventing Torsional Vibration Problems in Reciprocating Machinery', 2002.

[11] A. S. Mendes, P. S. Meirelles, and D. E. Zampieri, 'Analysis of torsional vibration in internal combustion engines: Modelling and experimental validation', *Proceedings of the Institution of Mechanical Engineers, Part K: Journal of Multi-body Dynamics*, vol. 222, no. 2, pp. 155–178, Jun. 2008.

[12] S. Kuroda, Y. Shimasaki, H. Igarashi, S. Maruyama, and T. Asaka, 'Development on digital filtering technology of crank speed measurement to detect misfire in internal combustion engine at high speed revolution', *JSAE Review*, vol. 16, no. 4, pp. 387–390, Oct. 1995.

[13] U. Kiencke, 'Engine misfire detection', *Control Engineering Practice*, vol. 7, no. 2, pp. 203–208, Feb. 1999.

[14] Z. Geng and J. Chen, 'Investigation into piston-slap-induced vibration for engine condition simulation and monitoring', *Journal of Sound and Vibration*, vol. 282, no. 3–5, pp. 735–751, Apr. 2005.